ANTIOXIDANTS & REDOX SIGNALING
Volume 4, Number 4, 2002

Forum Review

Heme Oxygenase: Evolution, Structure, and Mechanism

ANGELA WILKS

ABSTRACT

Heme oxygenase has evolved to carry out the oxidative cleavage of heme, a reaction essential in physiological processes as diverse as iron reutilization and cellular signaling in mammals, synthesis of essential light-harvesting pigments in cyanobacteria and higher plants, and the acquisition of iron by bacterial pathogens. In all of these processes, heme oxygenase has evolved a similar structural and mechanistic scaffold to function within seemingly diverse physiological pathways. The heme oxygenase reaction is catalytically distinct from that of other hemoproteins such as the cytochromes P450, peroxidases, and catalases, but shares a hemoprotein scaffold that has evolved to generate a distinct activated oxygen species. In the following review we discuss the evolution of the structural and functional properties of heme oxygenase in light of the recent crystal structures of the mammalian and bacterial enzymes. *Antioxid. Redox Signal.* 4, 603–614.

INTRODUCTION

HEME OXYGENASE (HO) catalyzes the rate-limiting step in the degradation of heme (iron-protoporphyrin IX irrespective of oxidation or ligation state) to biliverdin, which is subsequently converted to bilirubin in the presence of biliverdin reductase (BVR) (Fig. 1). The reaction requires the input of three molecules of oxygen and a total of seven electrons for the conversion of one heme molecule to biliverdin, carbon monoxide (CO), and iron (Fig. 1) (19, 29, 30). The transfer of electrons from NADPH to the mammalian HOs is mediated by cytochrome P450 reductase, the same reducing partner that is responsible for electron transfer to the cytochrome P450 enzymes (36, 60). HO regiospecifically cleaves heme at the α-*meso*-carbon to yield biliverdin IXα as the sole enzymatic product (45). Oxygen ($^{18}O_2$)-labeling studies and subsequent mass spectral analysis have determined that both oxygen atoms in biliverdin arise from molecular oxygen (46). Brown and co-workers further determined that three distinct oxygen molecules were involved in the reaction, the first in the conversion of heme to α-*meso*-hydroxyheme, the second in the formation of verdoheme, and the third in the final step from verdoheme to biliverdin (Fig. 1) (6, 7).

HO is highly unusual in that it uses heme as a substrate and cofactor for its own degradation, and is not therefore a hemoprotein in the classic sense of the cytochromes P450, peroxidases, or catalase enzymes. It is clear, however, from the nature of the reaction that HO shares a similar evolution of hemoprotein scaffolds that mediate oxygen activation. The elucidation of the HO mechanism will advance not only our understanding of oxidative heme cleavage, but also our knowledge of the relationship between structure and function in other hemoproteins.

SEQUENCE CONSERVATION WITHIN THE HO FAMILY

The amino acid sequences of the human HO-1 and HO-2 isoforms are ~42% identical, somewhat lower than the 80% identity between the human and rat HO-2 isoforms (24) (Fig. 2). The recently identified HO-3 has a much lower homology with either HO-1 or HO-2 but appears to be more closely related to HO-2 (25). Regions of high sequence identity are found in the amino acids corresponding to residues 125–150 and 11–40 in HO-1. A histidine (His-25) in the latter sequence has been identified as the proximal histidine to the heme (see following section).

Interestingly, the region of highest sequence identity, residues 125–150 in HO-1 and 144–169 in HO-2, corresponds

Department of Pharmaceutical Sciences, School of Pharmacy, University of Maryland, Baltimore, MD 21201-1180.

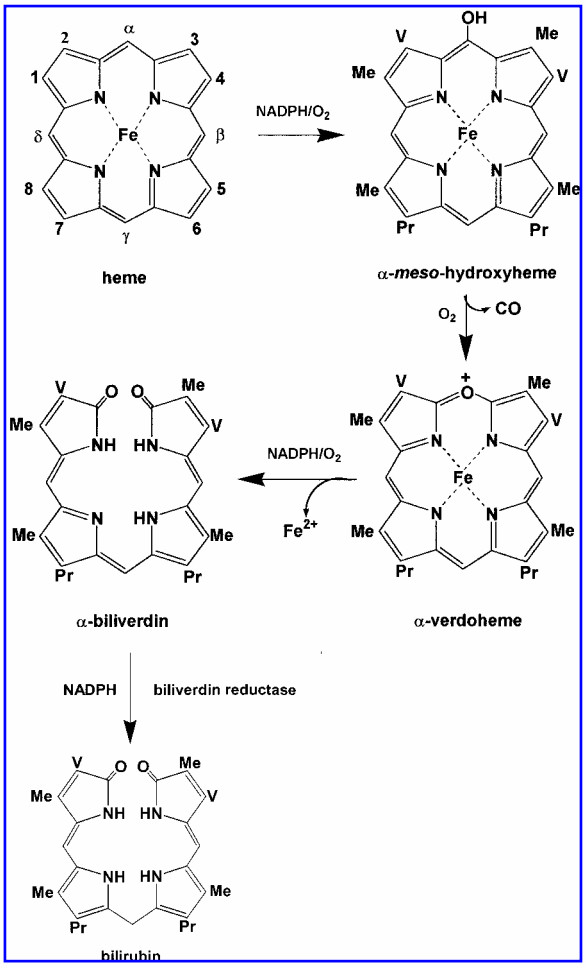

FIG. 1. Enzymatic conversion of heme to bilirubin by the combined action of HO and BVR. Abbreviations are as follows: Me, methyl (-CH_3); V, vinyl (-CH=CH_2); Pr, propionate (-CH_2-CH_2-COOH). The heme pyrrole carbons are labeled 1–8 and the *meso*-carbons α–γ.

to the sequence of the distal helix, which lies above the heme (see following section). This region was thought to be a fingerprint motif for the HO proteins (22), and further identification of HOs in the cyanobacteria and higher plants with a high degree of conservation within the distal helix supported this theory (3, 4). The identification and characterization of a HO (HmuO) from the heme-utilizing bacterial pathogen *Corynebacterium diphtheriae*, with 33% sequence identity and 70% homology to the human HO-1, again showed the highest identity in residues 122–145, corresponding to residues 125–150 in HO-1 (37, 54) (Fig. 2).

Most recently, we have characterized iron-regulated genes from *Neisseriae meningitides* (*hemO*) (62, 63) and *Pseudomonas aeruginosa* (*pigA*) (32) as HO enzymes. These pathogens have evolved to utilize the host's heme as an iron source, with the release of iron for further use by the pathogen being dependent on HO (32, 62, 63). In contrast to the *C. diphtheriae* enzyme, the amino acid sequences of *Pseudomonas* and *Neisseriae* show a much lower degree of sequence identity to previously characterized HOs. The low sequence identity (19–22%) is characterized by significant deletions and amino acid substitutions within previously conserved regions of the more well characterized HOs, particularly in the region corresponding to the distal helix (Fig 2). The only apparent conserved sequence within this region is the G-X-X-X-G motif corresponding to glycine residues 139 and 143 in HO-1 (Gly-116 and Gly-120 in HemO) with Leu-141 (Leu-119 in HemO) and Ser-142 (Ser-117 in HemO) being conserved within the sequence (Fig. 2). It is clear from the sequence alignments that with the exception of the previously mentioned motif and the proximal histidine, a clear picture of critical active-site residues required for catalytic activity and regiospecificity is limited.

STRUCTURAL STUDIES OF THE HUMAN HO-1 AND *Neisseriae meningitidis* HemO

Overall fold

It was anticipated that the crystal structures of a truncated soluble form of the human and rat HO-1 enzymes complexed with heme would provide significant insight into both the mechanism and regiospecificity of the HO reaction (38, 41). The structure of the human HO-1 lacking the terminal 55 amino acids, including a 23 C-terminal hydrophobic membrane anchor, has been refined to 1.5 Å (38). Despite the truncation of the protein, the activity and regiospecificity of the reaction were largely unaffected (38, 56). In addition, the first nine N-terminal residues as well as the last 10 residues of the truncated protein are not ordered in the electron density maps, and therefore a significant portion of the protein is not represented within this structure. More recently, we have solved the crystal structure of the soluble 24-kDa HemO from *Neisseriae meningitidis* to 1.5 Å (39). With the exception of the first eight N-terminal and three C-terminal amino acid residues, the complete protein sequence is ordered in the electron density maps. The first striking observation given the limited sequence identity between HO-1 and HemO is the high degree of structural conservation (Fig. 3A). The HO proteins have a novel fold primarily α-helical. The δ-*meso*-edge of the heme and the propionates are exposed at the molecular surface of the protein. Interestingly, the bacterial enzyme appears to have a "tighter" overall fold with the distal helix more closely approaching the heme. It is unclear at this point whether this is structurally or catalytically relevant, but it may be that the human HO-1 structure is slightly "loosened" up as a consequence of removal of the C-terminal domain. The C-terminus of HemO wraps back around toward the active site with Pro-206 being less than 4.0 Å from Asp-24 and Asp-27. The final three residues His-Arg-His of HemO were not ordered in the electron density map.

Heme pocket

The heme is sandwiched between two helices, more commonly referred to as the proximal and the distal helices. The proximal helix donates the histidine ligand, His-25 in HO-1 and His-23 in HemO (Fig. 3B). Thr-21 in HO-1 contacts the

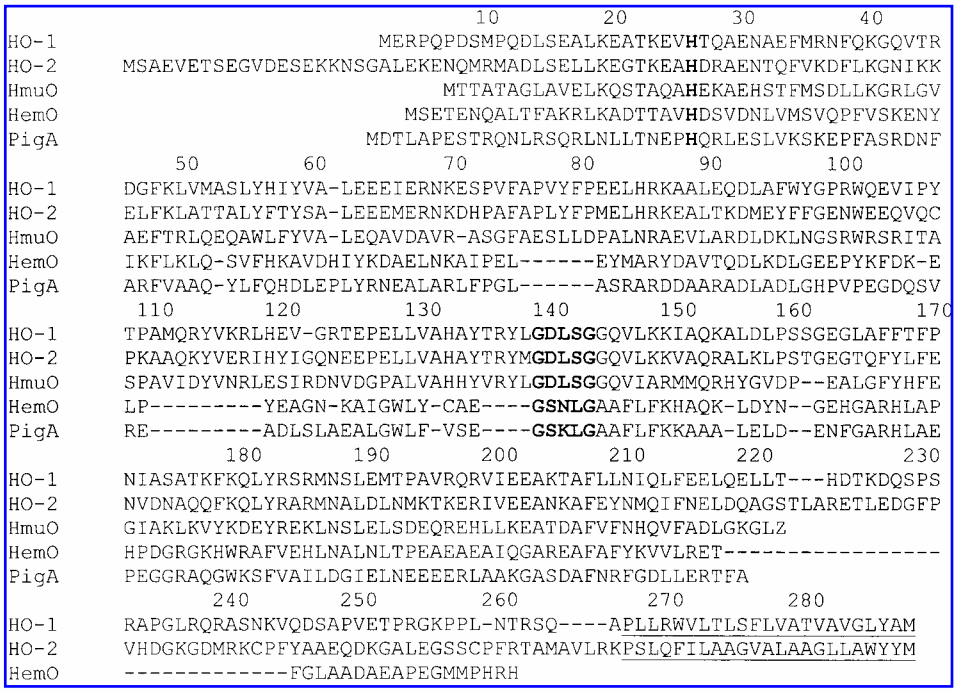

FIG. 2. Sequence alignment of the human and bacterial HOs. HO-1 and HO-2, human isozymes, HmuO, *Corynebacterium diphtheriae*, HemO, *Neisseriae meningitidis*, and PigA, *Pseudomonas aeruginosa*. Numbering is for the human HO-1 isozyme. The proximal His and the conserved glycine motif are shown in bold. The C-terminal membrane anchor of the human isozymes is shown underlined.

heme through a water molecule with the corresponding Thr-19 in HemO contacting the heme in the same manner. Additional contact residues with the heme include Ala-28 and Glu-29 of HO-1 corresponding to Val-26 and Asp-27 in HemO. HO-1 Glu-29 on the proximal side of the heme is close enough to form a hydrogen bond with the proximal histidine, whereas the corresponding Asp-27 at 5.1 Å is not close enough to hydrogen-bond to the proximal His. However, Asp-24 is 3.0 Å from the Nδ of His-23 and may fulfil the same role as Glu-29 in HO-1.

Resonance Raman spectroscopic studies on the human HO-1 indicate that the resting state ferric heme-HO-1 complex is a neutral imidazole with no imidazolate character (42, 43). We have recently characterized the ferric heme-HemO complex by resonance Raman spectroscopy (unpublished results), and as in HmuO the conserved glutamate, corresponding to Glu-29 and Glu-24 in HO-1 and HmuO, respectively, shows no evidence of a hydrogen-bond interaction in the resting state enzyme (52). It must be emphasized, however, that a more detailed spectroscopic investigation is required to determine if the proximal His is neutral throughout the reaction from heme to biliverdin. The H25A mutant of HO-1 is inactive, although activity is rescued on addition of exogenous imidazole (57). In contrast, the *C. diphtheriae* HmuO H20A mutation in the absence of exogenous ligand converts heme to verdoheme, and on reconstitution with imidazole reacts to give biliverdin as the final product (52). The reason as to why the H20A HmuO mutant, in contrast to the H25A HO-1 construct, can catalyze the initial hydroxylation of the heme is not yet understood. The reaction of the H20A mutant generates the Fe^{II}-verdoheme complex as evidenced by the band at 650 nm in the visible spectrum, which is similar to that reported for the CO-Fe^{II}-verdoheme complex (16). In contrast, Fe^{III}-verdoheme complexes have a band at 690 nm (20). Interestingly, studies on a H63M mutant of cytochrome b_5 concluded that the protein was capable of carrying out the coupled oxidation of heme to verdoheme, but did not proceed to biliverdin (33). The termination of the reaction at the verdoheme stage was thought to occur as a result of a coordination of Met-63 to the Fe^{II}-verdoheme intermediate. It has previously been observed in coupled oxidation systems that high-affinity ligands binding to both the fifth and sixth coordination sites of verdoheme inhibit the reaction to biliverdin (34). This is consistent with inhibition of Fe^{II}-verdoheme conversion to biliverdin by CO, which confirms that only five-coordinate verdoheme complexes are capable of undergoing further oxidation to biliverdin (35). It is possible that the reaction of H20A HmuO is inhibited either by back inhibition of CO released as a consequence of oxidative cleavage, or by coordination of a protein residue to the heme. This, however, does not explain the initial observation that α-*meso*-hydroxylation occurs in the absence of the proximal ligand in the heme-H20A HmuO complex, whereas in the heme-H25A HO-1 complex no activity is observed. Resonance Raman studies on the heme-H20A HmuO complex have shown that the ligand to the heme is similar in nature to that of H25A HO-1, and most likely arises from a water or interaction with a Glu or Asp (52). Indeed, recent unpublished magnetic circular dichroism (MCD) studies have indicated that the ligand to the heme in H20A HmuO is somewhat weaker than that in

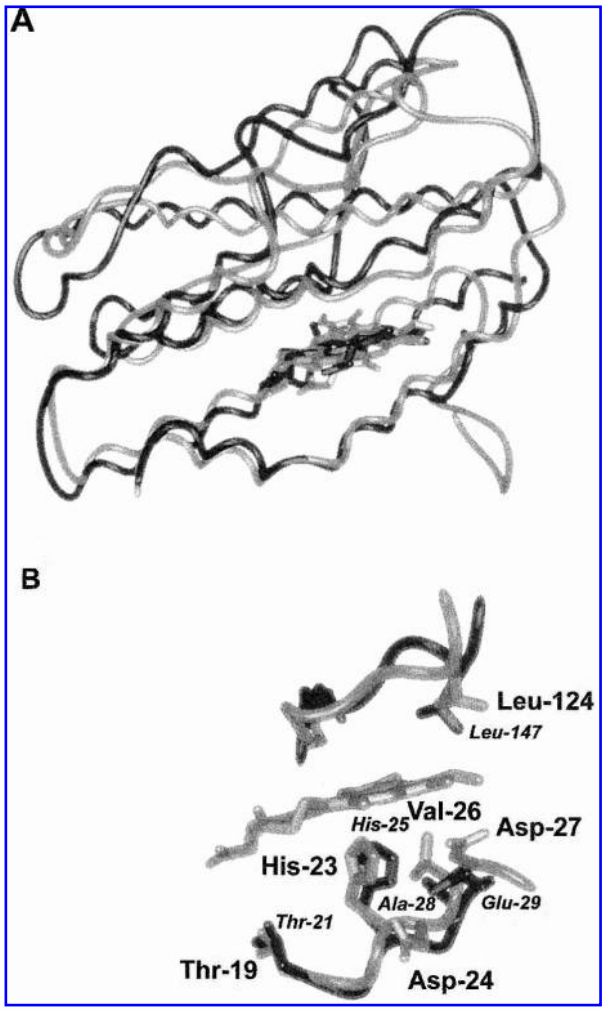

FIG. 3. Overall structure and comparison of the active site of human HO-1 and *Neisseriae meningitidis* HemO. **(A)** Overall structure of HO-1 (dark gray) and HemO (light gray) (38, 39). **(B)** Conserved active site residues of HemO (light gray and HO-1 (dark gray) (HO-1 residues are shown italicized).

H25A HO-1, but again is most consistent with a Glu or Asp residue, as previously described for the heme-H25A HO-1 complex (31). In addition, we have recently constructed the H23A HemO mutant, and in contrast to both the HO-1 and HmuO proximal mutants, this mutation resulted in a heme-H23A HemO complex that had no activity in the presence or absence of imidazole (unpublished results). Indeed, the heme-H23A HemO complex gave no evidence of imidazole coordination to the heme even at concentrations 1,000–10,000-fold higher than those used in previous studies of the heme-H20A HmuO complex. We are further characterizing the heme-H23A HemO complex by MCD and resonance Raman spectrophotometric techniques.

One possible explanation for the inability of imidazole to coordinate to the bound heme may be found in the smaller solvent-accessible surface area of the distal heme-binding pocket (see below). These results suggest that subtle changes within the active-site polarity and/or geometry may account for the different reactivity of the proximal mutants, and factors that position the heme in a suitable orientation and environment for hydroxylation may not necessarily involve the proximal histidine. As will be outlined below, the heme propionate interactions may be more critical in defining heme binding and, to some extent, reactivity.

Of the four heme *meso*-edges, only the δ-*meso*-edge is exposed at the surface of the protein (Fig. 4). The other three edges are buried within the protein with the α-*meso*-edge in both HO-1 and HemO butting up against a hydrophobic wall of residues including Met-34, Asn-210, and Phe-214 in HO-1 with the corresponding Val-30, Tyr-184, and Leu-188 in HemO.

Somewhat surprisingly, the distal pocket of the heme-HemO complex is significantly smaller than that of HO-1, having a solvent-accessible volume of 7.5 Å as compared with 53.5 Å for the more closed form of the heme-HO-1 complex. It is apparent from the sequence alignment of HemO and HO-1 (Fig. 2) that there are significant deletions in the distal helix region of HemO that could account for the difference in the solvent accessible volume of the distal pocket. The distal helix has a kink of ~50° directly over the heme provided by the glycines of the highly conserved sequence ^{139}Gly-Asp-Leu-Ser-Gly-Gly^{144} in HO-1 and ^{116}Gly-Ser-Asn-Leu-Gly-Ala^{121} in HemO (Fig. 3). This kink in the helix is thought to provide the flexibility required for binding of the substrate (heme) and release of the product (biliverdin). The helix closely approaches the heme with direct backbone contacts from Gly-139 and Gly-143 in HO-1. Recently, Ortiz de Montellano and co-workers have shown that mutation of Gly-139 or 143 resulted in a loss of oxygenase activity and an in-

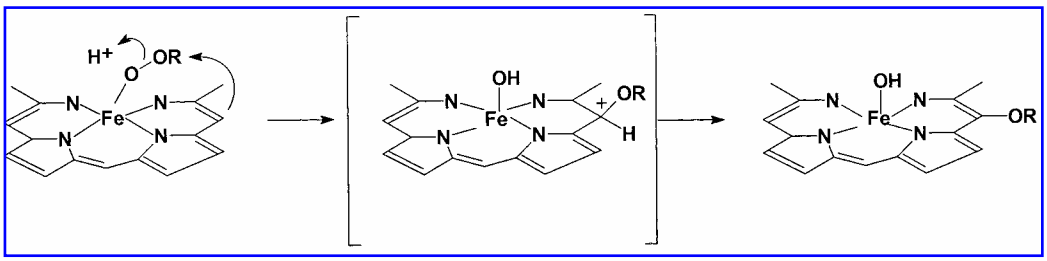

FIG. 4. Electrophilic oxidation of the heme by HO. H_2O_2 as the oxidant R = H with α-*meso*-hydroxyheme as the product; ethyl hydroperoxide as oxidant R = -CH_2CH_3 with α-*meso*-ethoxyheme as the product.

crease in peroxidase activity (21). In all of the Gly-139 mutants (with the exception of the G139A mutant), the water ligand in the resting state was lost giving rise to a pentacoordinate species, as determined by resonance Raman spectrophotometric studies. The authors concluded that these residues are critical in maintaining an environment conducive to oxygenase activity, and the key role of the HO protein environment may be to suppress the formation of a ferryl species.

The other contact residue donated from the distal helix conserved in HemO is Leu-124 corresponding to Leu-147 in HO-1. The polar residues closest to the heme on the distal face of HO-1 have largely been replaced in HemO; Ser-142 is replaced by Leu-119 at the γ-edge, Arg-136 is replaced by Ala-114, whereas Ser-117 and Asn-118 largely occupy the space of Asp-140 in the HO-1 structure. In the human enzyme, a cluster of polar residues near pyrrole B including Asn-210, Arg-136, and Asp-140 appear to form a network of polar residues with a second tier of residues Tyr-58 and Tyr-114. In HemO, Ser-117 appears to occupy the position of a water molecule that is hydrogen-bonded to Asp-140 in HO-1. The polar influence over pyrrole B in HemO is largely determined by His-141 and His-53 replacing Phe-166 and Tyr-58 of HO-1.

Although the residues involved in the hydrogen-bonding network of HO-1 are far enough from the α-*meso*-carbon not to be directly involved in the reaction, they contribute to the polar nature of the heme-binding pocket. It was proposed that these residues may be important in both ligand discrimination and regiospecificity. In an effort to understand the role of this hydrogen-bonding network, Ortiz de Montellano and coworkers have replaced Asp-140 in the active site with a number of residues that decreased the formation of biliverdin and increased the peroxidase activity of the enzyme (18). They concluded that replacement of Asp-140 with Ala, Phe, His, or Asn disrupted oxygen binding resulting in a much smaller proportion of the Fe^{III}-O-OH intermediate being directed to the α-*meso*-carbon, with the resulting heterolytic O-O bond cleavage yielding the ferryl species.

The critical nature of Asp-140, however, remains unclear given that it falls between the positions occupied by Ser-117 and Asn-118 in HemO. Interestingly, the authors note that the Asp-140 to Asn mutation is the only mutation in which the resulting protein retains substantial six-coordinate character as well as the ability to convert heme to Fe^{III}-verdoheme, whereas the conversion of Fe^{III}-verdoheme to biliverdin is completely inhibited.

Mutations that disturb the overall structure of the distal helix result in a decreased efficiency in catalysis, particularly mutations within the glycine motif that provides the flexibility to the distal helix. The degree of complexity in maintaining the structural integrity required for catalysis, as implied from the lack of overall conservation within the distal helix, appears to go beyond a single residue and most likely involves a number of dynamic parameters not evident from the present structural data.

Regiospecificity

Propionate charge interactions are critical in binding and correctly orienting the α-*meso*-carbon of the heme for hydroxylation (38). Residues in close proximity to the propionates in HO-1 are Lys-18, Lys-22, Lys-179, and Arg-183, as well as Tyr-134. In the heme-HemO complex, only Lys-16 and Tyr-112 corresponding to Lys-18 and Tyr-134 are absolutely conserved in the structure. Lys-22 is replaced by Thr-20, and Trp-53 largely fills the space occupied by Arg-183 and Lys-179. Recent mutagenesis studies on Arg-183 have suggested that this residue is involved in orienting the heme within the active site through direct hydrogen bonding to the propionate group (61). The authors suggest that the appearance of the δ-isomer as a product of the reaction is a consequence of a new hydrogen-bonding network involving Glu-183 and Lys-179 concomitant with disruption of a hydrogen bond between Lys-179 and Ser-142. The authors further note that the shift in pK_a of the dissociatable water from 7.9 to 9.2 is indicative of such a change. However, it must be noted that neither Lys-179 nor Arg-183 is conserved in HemO. It therefore remains of great interest to understand the role of both Tyr-134 and Lys-18 in binding and regiospecificity. The significance of the ionic/hydrogen bonding interaction of the propionates with Lys-16 and Tyr-112 in HemO is highlighted by the recent finding that the Pseudomonal HO (PigA) in which these residues are replaced by Asn-18 and Phe-116 oxidatively cleaves heme at the β-meso-carbon (32). The role of these residues in regioselectivity is currently being investigated in our laboratory. The isolation of a HO with an altered regioselectivity will allow a more in-depth study of the steric and electronic factors involved in the regioselectivity of heme cleavage.

Although the structure of both HO-1 and HemO support the role of the protein scaffold in the regiospecificity of the HO reaction, it is clear that electronic factors are also of critical importance. Early paramagnetic two-dimensional (2D) nuclear magnetic resonance (NMR) studies on HO-1 revealed that the heme binds in two orientations that differ by 180° around the α/γ axis (12). In addition, the contact shift patterns to the heme suggested an unusual electronic structure characterized by large changes in the delocalized spin density for the two peripheral carbons within a given pyrrole, rather than differences between adjacent pyrroles more commonly found in hemoproteins such as myoglobin. Originally, it was proposed that the electronic perturbation arose from an anionic side chain close to the α-*meso*-carbon. No such anionic group is evident from the crystal structure, however, and it is unclear at the present time the role such an electronic perturbation would play in regiospecificity and reactivity.

A further complication in the steric versus electronic control of regiospecificity comes from enzymatic studies with *meso*-methylhemes (49). In these studies, the electron-donating methyl group essentially mimics the anionic residue reported to confer the unique electronic structure on the heme-HO-1 complex. Oxidation of the α-*meso*-methylheme HO-1 complex somewhat surprisingly yielded biliverdin IXα (51). In subsequent studies with a ^{13}C-labeled *meso*-methylmesoheme, the authors ruled out the formation of CO, acetaldehyde, or acetic acid as a product of the cleavage, but have not yet successfully identified the fragment (48). Further studies with the β, δ, and γ-*meso*-methyl isomers indicated that the position of the electron-donating group played a significant role in determining the regiospecificity of cleavage (49). The γ-*meso*-methylmesoheme was exclusively oxi-

dized at the γ-position to γ-mesobiliverdin, the δ-*meso*-methyl isomer at both the δ- and α-position, and the β-*meso*-methylmesoheme was a poor substrate, even though the α-position was not blocked. Although these studies appear to support a role for electronic factors in the control of regiospecificity, it is also possible that the binding of a puckered porphyrin would induce structural changes within the active site. Some structural perturbation may be suggested by the different reactivities of the δ- and β-*meso*-methylmesohemes. It is difficult to rationalize these results given that the rotation of the heme around the α/γ-axis observed in early NMR studies would suggest the cleavage patterns should be similar if 180° rotation occurred similarly for the *meso*-methylmesohemes. It is also possible, however, that substitutions at the β- and δ-*meso*-carbons would restrict the heme to binding in a single orientation. To address the possibility that perturbations of the porphyrin structure were responsible for the cleavage pattern, the authors synthesized the α-*meso*-formylmesoheme, which differs only from α-*meso*-methylmesoheme in that the former is electron-withdrawing, and the latter electron-donating (50). In contrast to the α-*meso*-methylmesoheme in which oxidation occurred at the site of the substitution, the α-*meso*-formylmesoheme is cleaved at a non-formyl-substituted site at either the β- or δ-position. It is clear from the above studies that a mechanism is required that reconciles the electronic factors with the structural evidence that steric as well as polar interactions of the bound Fe-O-O with the surrounding environment play a significant role in the regiospecificity of heme cleavage.

A detailed 2D NMR characterization of the heme pocket revealed a cluster of nine aromatic residues that form part of the heme-binding pocket (11). The heme was thought to be bound with pyrroles A (1-methyl, 2-vinyl), B (3-methyl), and D (8-methyl) buried toward the interior of the protein, and pyrroles C (5-methyl, 6-propionate) and parts of pyrrole B (4-vinyl) and D (7-propionate) exposed to solvent. These assignments again have not been consistent with the crystal structure, possibly because of the 180° rotation of the heme about the α/γ axis (12).

A labile proton within the active site thought to arise from a Tyr or His within van der Waals contact of the heme was proposed to be the distal base forming a hydrogen bond to the coordinated water. However, mutation of all of the conserved His and Tyr residues caused no loss in activity, or loss of the distal water ligand. These mutagenesis experiments are consistent with the crystal structure in which no active-site residue appears to be coordinated to the distal water ligand. Despite the obvious discrepancies between the 2D NMR data and the crystal structure, it is obvious that the protein plays an important role in modulating the reactivity of the heme, which cannot be assessed from the static structure.

The structural characterization of the heme-HO-1 complex revealed two structures. In one of the structures, the distal helix is packed more tightly to the heme with the Cα of Gly-139 at a distance of 3.7 Å from the heme, in the second, the distal helix is less tightly packed with the Cα of Gly-139 at 5.7 Å from the heme. The heterogeneity attributed to the distal helix as judged by the root mean square deviation and high thermal factors may well have mechanistic implications because it would allow for easy opening of the active site for binding of substrate and release of product, while the close proximity of the distal helix to the heme allows greater control of reactivity and regiospecificity. It must also be pointed out that this structure represents only two states that may not represent the most open and closed forms. The more recent HemO structure further supports this as evidenced by the close proximity of the distal helix to the heme.

Further clarification of many of the unresolved questions arising from the crystal structures of both HO-1 and HemO awaits structural characterization of reaction intermediates in the conversion of heme to biliverdin, as well as heteronuclear NMR studies directed at solving the solution structure of HO.

Ligand discrimination

Perhaps the most interesting aspect of HO is how it has evolved to discriminate between O_2 and CO. The O_2 affinities of ferrous heme-HO-1 and HO-2 are 30–90-fold higher than those of mammalian myoglobins (27). Comparison of the dissociation constants indicates a much slower rate of dissociation from HO than the globins. In contrast, the affinities for CO in HO are only sixfold higher than those for oxygen in contrast to the much higher affinities for CO compared with O_2 in the globins. Thus, the ratios of K_{CO}/K_{O_2} are ~5.4 and ~25 for HO and the globins, respectively (27, 40). Two possible explanations for the decrease in O_2 dissociation and CO affinity are suggested by the crystal structure of HO-1. Although there is no distal base such as histidine to coordinate directly to the bound oxygen, there is an ordered set of water molecules within the active site that may be involved in a hydrogen-bonding network with the oxygen. Indeed, electron paramagnetic resonance (EPR) studies on the oxy-cobalt-HO-1 have shown solvent deuterium isotope shifts consistent with the oxygen involvement in a hydrogen-bonding interaction (10). Secondly, the presence of a hydrophobic channel in close proximity to the α-*meso*-edge may promote CO release through this channel rather than into the more polar heme pocket, effectively reducing the inhibitory concentration of CO. The absence of such a hydrophobic channel in the structure of HemO has interesting implications for both substrate specificity (see following section) and CO discrimination.

SUBSTRATE SPECIFICITY

The studies that have been carried out in regard to substrate specificity have primarily been carried out with the mammalian HO-1 isozymes. HO is highly specific for the heme propionates at positions 6 and 7, but is much less stringent to variations at positions 1–4 (see Fig. 1 for numbering). Exchanging the positions of the methyl and propionate groups at positions 5–8 or shortening the length of the propionates results in substrates that are no longer viable (8, 9, 47). In contrast, a large number of substituents are acceptable at one or more of the positions 1–4, including chain lengths of up to 12 carbons, both polar and nonpolar. These studies have largely been verified with the recent crystal structures of HO-1 and HemO, where a number of Arg and Lys residues are located in close proximity to the heme propionates (38, 39). The heme orientational heterogeneity observed in NMR stud-

ies of the human heme-HO-1 complex also supports the propionates being essential for heme binding as 180° rotation around the α/γ axis would simply result in the propionates switching position in the two orientations. The position of the α-*meso*-edge would be unaffected by this heterogeneity and the apparent nonspecificity for substituents at positions 1–4 is suggestive of an active-site structure that could accommodate more complicated hemes that may arise physiologically, for example, from degradation of proteins such as cytochrome *c* (15). Indeed, the presence of a hydrophobic channel in HO-1 may accommodate hemes with hydrophobic substituents. The absence of such a channel in the bacterial HemO may reflect a fundamental physiological difference in that receptor-mediated heme uptake is most likely restricted to protoporphyrin IX.

MECHANISM OF HO

Nature of the activated oxygen and α-meso-*hydroxylation*

The first step in the catalytic turnover of heme is the reduction of the ferric (Fe^{III})-heme-HO-1 complex to the ferrous state by NADPH-cytochrome P450 reductase. Reduction of the ferric complex to the ferrous state can be monitored in the presence of CO with formation of the distinctive ferrous (Fe^{II})-CO heme-HO-1 complex (58, 59). On reduction of the iron to the Fe^{II} oxygen is bound to give the Fe^{II}-O_2 complex with a Soret maximum at 410 nm, which bears a striking resemblance to the Fe^{II}-O_2-myoglobin spectrum (60). Recent resonance Raman studies on the isotopically labeled Fe^{II}-O_2 complex have shown an isotope shift pattern that suggests the oxygen is highly bent, with the terminal oxygen closely approaching the α-*meso*-carbon (44). The highly bent state of the bound dioxygen contrasts sharply with the more linear geometry of the Fe^{II}-O_2 myoglobin complex. The authors concluded based on the similarity of the His-Fe stretching frequencies in both the Fe^{II}-O_2 myoglobin and Fe-O_2-cobalt HO-1 complexes that the effect is due to steric factors within the heme-binding pocket, a conclusion consistent with the recent crystal structures (38, 39). In addition, hydrogen-bonding interactions within the polar environment created by the ordered water molecules in the vicinity of the α-*meso*-edge may facilitate the bent geometry required in directing the dioxygen toward contact with the α-*meso*-carbon.

The dioxygen geometry has obvious implications for the hydroxylation of the α-*meso*-heme edge. Once the Fe^{II}-O_2 complex is formed, a second electron transfer to the heme reduces the Fe^{II}-O_2 complex to the activated peroxide intermediate. At this stage, HO differs significantly from the more well characterized heme enzymes that undergo heterolytic cleavage of the O-O bond to yield the active ferryl complex $(Fe\text{-}O)^{3+}$ rather than a peroxide intermediate. The addition of hydrogen peroxide (H_2O_2) supports the hydroxylation of the α-*meso*-carbon to yield α-*meso*-hydroxyheme, which in the presence of oxygen is directly converted to verdoheme (13, 53). Therefore, H_2O_2 is equivalent to a molecule of oxygen and two electrons in the reaction of heme to verdoheme, but does not support the catalytic conversion of verdoheme to biliverdin (53). Anaerobic addition of H_2O_2 to the Fe^{III}-heme HO-1 complex produced an intermediate stable in the absence of oxygen (20). This intermediate is identical, as determined by absorption spectroscopy and resonance Raman, to that reported for the synthetic α-*meso*-hydroxyheme HO-1 complex (23).

The nature of the peroxide species involved in hydroxylation of the heme has been studied in more detail with the acyl and alkyl peroxides (53). Reaction of the Fe^{III}-heme-HO-1 complex with *meta*-chloroperbenzoic acid generated a ferryl complex that did not support hydroxylation. Similarly, the larger alkyl peroxides, such as *tert*-butyl hydroperoxide and cumene hydroperoxide, formed a ferryl species with no evidence of heme modification. The reaction with the much smaller ethyl hydroperoxide gave the most interesting and informative result (55). Although ethyl hydroperoxide also gives rise to a ferryl species, reduction of the peroxo intermediate to prevent nonspecific degradation of the heme, followed by HPLC isolation of the heme, identified a fraction of the heme that had been modified. The modified heme was characterized by absorption, NMR, and mass spectrophotometric techniques as α-*meso*-ethoxyheme (55). The formation of α-*meso*-ethoxyheme paralleled that of α-*meso*-hydroxyheme, the first step in the enzymatic reaction. The α-*meso*-ethoxyheme is stable compared with α-*meso*-hydroxyheme, which is rapidly deprotonated to verdoheme as part of the normal reaction pathway. These experiments highlighted one important aspect of the HO reaction and that is the nature of the active peroxide. The reaction specifically rules out a mechanism by which the terminal oxygen of a peroxo anion (Fe^{III}-O-O^-) adds as a nucleophile to the α-*meso*-carbon because in the ethyl hydroperoxide reaction the terminal oxygen is blocked. These results therefore imply that the Fe^{III}-O-OH intermediate undergoes electrophilic addition at the α-*meso*-edge, a mechanism that supports the data from both the studies with H_2O_2 and ethyl hydroperoxide (Fig. 4).

A series of elegant experiments utilizing electron-nuclear double resonance and EPR spectroscopy techniques were carried out on the cryogenically reduced Fe^{II}-O_2 HO-1 complex (5). In these studies, direct demonstration of a one-electron reduction of the Fe^{II}-O_2 HO-1 complex identified α-*meso*-hydroxyheme as a true intermediate in HO catalysis, and corroborated the hydroperoxide species as the activated oxygen in HO substrate hydroxylation.

In this respect, the reactivity of HO in which the activated oxygen species is the hydroperoxide (Fe^{III}-O-OH) represents a new class of hemoprotein reactivity distinct from that of the more common ferryl species $(Fe\text{-}O)^{3+}$ of the cytochromes P450 and peroxidases. The less characterized peroxo-anion (Fe-O-O^-) species that directly reacts as a nucleophile with highly electrophilic substrates also has precedent in the literature as a currently accepted mechanism for the carbon–carbon bond cleavage reactions associated with cytochrome P450 enzymes such as lanosterol-14α-demethylase and sterol 17-lyase (17). One of the more challenging aspects in the future will be in understanding the structural and electronic factors that contribute to these unique hemoprotein manifolds.

Conversion of α-meso-*hydroxyheme to verdoheme*

The conversion of α-*meso*-hydroxyheme to verdoheme is an oxygen-dependent process as evidenced from the reaction with H_2O_2 or on reconstitution with synthetic α-*meso*-hydroxyheme where, in the absence of oxygen, α-*meso*-hydroxyheme is a stable intermediate (20, 23). Addition of oxygen to the anaerobic α-*meso*-hydroxyheme complex results in the appearance of an organic radical in the EPR spectrum with a signal at g = 2.008 and a rhombic component at g = 6.07 and 5.71 characteristic of the Fe^{III} species (20). The addition of CO to the anaerobic system results in the loss of the Fe^{III} component of the EPR spectrum and an increase in the radical signal at g = 2.004 (23). It can be concluded that the presence of CO drives the reaction in the direction of the radical intermediate and that in the presence of O_2 the radical species is in equilibrium with the Fe^{III} species (Fig. 5). Although it is largely agreed that the Fe^{III}-*meso*-hydroxyheme is in equilibrium with the Fe^{II} radical form, some question remains on the requirement of reducing equivalents for the conversion of α-*meso*-hydroxyheme to verdoheme. In studies with synthetically reconstituted apo-HO-1 and α-*meso*-hydroxyheme, it has been reported that the formation of verdoheme required input of a further reducing equivalent as well as O_2 (23, 28). Liu *et al.*, however, reported that only the addition of oxygen was required for the conversion of the H_2O_2-generated α-*meso*-hydroxyheme to verdoheme (20). This is in agreement with earlier studies on model systems in which α-*meso*-hydroxyheme-reconstituted myoglobin is converted to verdoheme without the addition of reducing equivalents (35). There is no question that the conversion of Fe^{III}-verdoheme to Fe^{II}-verdoheme requires an electron, but the observation that Fe^{III}-verdoheme accumulates in high yields in the H_2O_2-driven reaction in the presence of O_2 clearly indicates that the electron is not required at this step of the reaction. Under physiological conditions in the presence of NADPH and cytochrome P450 reductase, Fe^{III}-verdoheme does not accumulate and is rapidly converted to Fe^{II}-verdoheme. There are two separate steps at which the electron may be introduced, either following formation of Fe^{III}-verdoheme in the formation of Fe^{II}-verdoheme (as shown), or prior to CO elimination directly forming Fe^{II}-verdoheme (Fig. 5) (20, 29, 30).

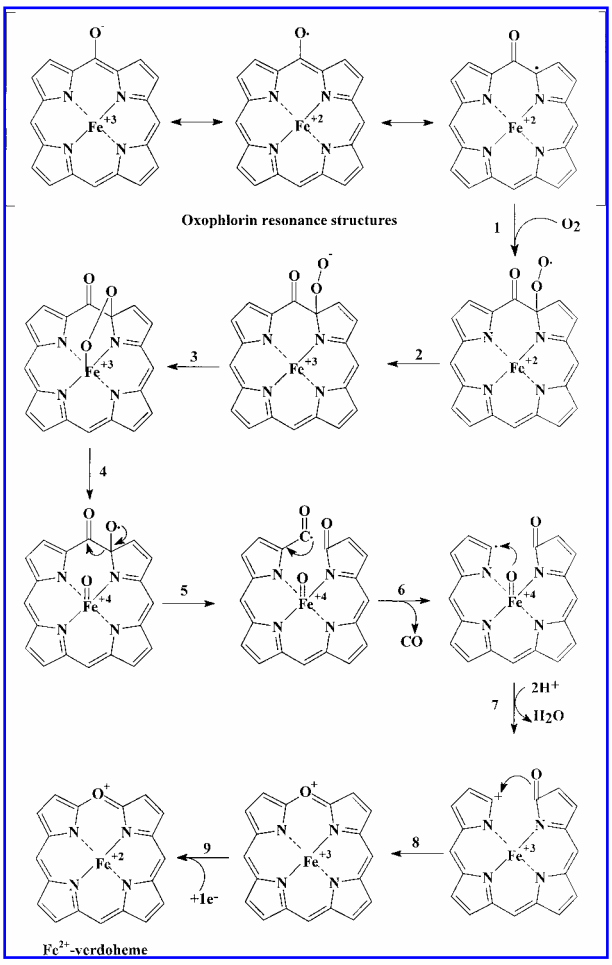

FIG. 5. Proposed mechanism for the conversion of α-*meso*-hydroxyheme to Fe^{II}-verdoheme. α-*meso*-Hydroxyheme is shown deprotonated. Adapted from reference 48.

Ortiz de Montellano has proposed two alternative mechanisms by which oxygen may react to give the peroxy-radical intermediate following deprotonation of α-*meso*-hydroxyheme to the oxophlorin (Fig. 5) (29, 30). The oxygen may react directly with the iron of the Fe^{II} intermediate, or at the porphyrin edge following internal electron transfer from the iron to give the Fe^{III}-hydroperoxy species. Either of these species would give rise to an unstable ferryl alkoxy radical with the consequent release of CO as a result of carbon–carbon bond cleavage. The resulting unstable carbon radical is then presumably internally oxidized to the cation by electron transfer to the ferryl species (Fig. 5).

Although it must be highlighted that none of the intermediates beyond the addition of oxygen to the porphyrin radical species have been identified spectrally, the mechanism provides a reasonable explanation of the steps involved in CO release and verdoheme formation.

Verdoheme to biliverdin

The final stage of the HO catalyzed reaction, and perhaps the least well understood, is the conversion of verdoheme to biliverdin. Early $^{18}O_2$-labeling studies on the reconstituted HO-1 system provided an important foundation for the mechanism of oxygen insertion (6, 7). Under a partial atmosphere of $^{16}O_2/^{18}O_2$, one atom each of ^{18}O and ^{16}O are incorporated into the final biliverdin product. The incorporation of two atoms of oxygen from separate oxygen molecules indicates that the reaction occurs solely by oxidation and not via a hydrolytic mechanism. Studies of verdoheme complexes in model systems had previously determined that formation of biliverdin required incorporation of molecular oxygen (34).

One important distinction with the utilization of H_2O_2 instead of NADPH-cytochrome P450 reductase is the inability of the reaction to proceed beyond verdoheme; indeed, the presence of excess H_2O_2 results in the nonspecific degradation of the heme to mono- and dipyrroles (53). This suggests that formation of Fe^{III}-verdoheme yields an intermediate in a higher oxidation state than is required for further reaction.

Presumably, the formation of biliverdin from verdoheme requires a two-electron reduction precluding H_2O_2 from carrying out the final step in the reaction. A hypothetical mechanism has been proposed by Ortiz de Montellano to account for these observations (Fig. 6) (29, 30). In this scenario, reduction of the Fe^{III}-verdoheme to the Fe^{II} state, binding of dioxygen, and a second one-electron reduction would give an intermediate formally equivalent to that obtained on reaction with H_2O_2 (steps 1 and 2 in Fig. 6). Following dioxygen bond cleavage to give an alkoxy radical or anion, the subsequent ring cleavage and two-electron reduction would give rise to the final Fe^{III}-biliverdin product. An alternative pathway may involve the stepwise addition of molecular oxygen to the porphyrin edge (step 3 in Fig. 6), whereas reaction with H_2O_2 may result in side reactions that give alternative products. It is also unknown at this time at which step in the pathway the two electrons required to produce Fe^{III}-biliverdin would be delivered.

The final step in the complete HO-dependent reaction is the conversion of Fe^{III}-biliverdin to Fe^{II}-biliverdin. This step in the pathway has important implications for the subsequent release of biliverdin and its conversion to bilirubin by the action of BVR. It had been suggested from early coupled oxidation studies, in which the final product is Fe^{III}-biliverdin, that Fe^{III}-biliverdin is not a substrate for BVR. The HO reaction with NADPH-cytochrome P450 reductase produces free biliverdin that is reduced quantitatively to bilirubin (59). More recently, Liu and Ortiz de Montellano have confirmed that the rate-limiting step in the enzymatic degradation of heme to biliverdin, in the absence of BVR, is biliverdin release (19). In the presence of BVR, the rate- limiting step in the single turnover studies was the conversion of Fe^{II}-verdoheme to Fe^{III}-biliverdin. One possible factor that may contribute to biliverdin release is direct protein–protein interaction of BVR with the biliverdin-HO-1 complex that somehow facilitates allosteric release of the product. The recent crystal structure of the BVR, although not directly addressing this question, does not preclude a physical interaction that may allosterically promote transfer of biliverdin from HO to BVR (14). Indeed, just as the propionate groups of the heme are important in binding and orienting the heme within HO-1, the presence of a number of Arg and Lys residues in BVR are ideally situated for interaction with the propionates of the resulting biliverdin (14). Interestingly, this exposed surface of the BVR protein is also somewhat electronegative, and may directly interact with the more electropositive face surrounding the exposed heme edge in the heme-HO-1 complex (38, 41).

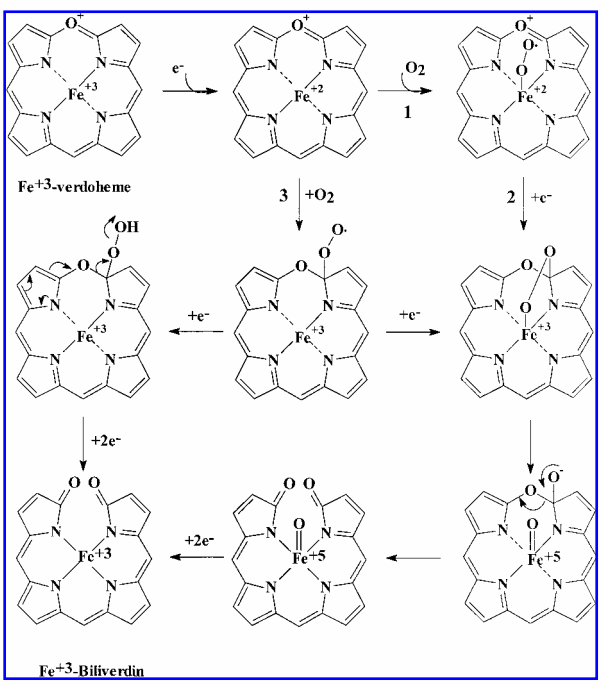

FIG. 6. Hypothetical scheme for the conversion of Fe^{II}-verdoheme to Fe^{III}-biliverdin. Two alternatives are shown that differ in the step at which electrons are introduced into the system. Adapted from reference 48.

Although such intensive and informative kinetic studies have implicated certain steps in the HO reaction as being rate-limiting, it is important to remember that the physiological conditions under which the reaction takes place may be somewhat different from those of the *in vitro* systems. Firstly, the rate of the overall reaction is somewhat sensitive to the ratio of NADPH-cytochrome P450 reductase to HO-1; secondly, the oxidation state of the heme available physiologically is not known and this may have consequences for the overall rate of the reaction.

In our recent studies on the bacterial HOs, we have found that, like the mammalian enzymes, in the presence of ascorbate the final product of the reaction is Fe^{III}-biliverdin, which is not a substrate for BVR (54, 63). The HmuO, HemO, and PigA enzymes from *C. diphtheriae*, *N. meningitidis*, and *P. aeruginosa*, respectively, show activity on reconstitution with the human cytochrome P450 reductase system. In all cases, however, the final product is Fe^{III}-biliverdin, which is not released from the active site in the absence of iron chelators or acidification of the reaction. Chu *et al.*, however, have recently reported that a recombinant HmuO generated from a synthetic gene construct generates biliverdin as the final product of the reaction, the Fe^{II} iron presumably being released (2). At this point, we do not understand the reported differences for the recombinant and natural gene products of HmuO, but in no HO system previously described has ascorbate supported the conversion of Fe^{III}-biliverdin to Fe^{II}-biliverdin. At the present time, we have not identified the endogenous electron donor for any of the bacterial HOs thus far characterized.

An interesting question arises when considering the nature of biliverdin metabolism in bacterial pathogens: what is the fate of the biliverdin? It is unlikely that biliverdin is converted to bilirubin as in mammalian systems, where such a process evolved for physiologically distinct reasons, primarily placental transport and possibly as a lipid-soluble antioxidant in protection from free-radical damage (26). The sole function of biliverdin in cyanobacteria, algae, and higher plants is as a biosynthetic precursor for the synthesis of the light-harvesting bilin pigments (1). In the bacterial pathogens, the primary reason for cleavage of the heme macrocycle appears to be in the acquisition of iron and therefore biliverdin may only reflect a waste product of this reaction. It

is possible that biliverdin is pumped out of the cells by a non-specific outer-membrane transporter or that it is further degraded and utilized as a carbon and/or nitrogen source. Although this question still remains, biliverdin does not appear to be toxic to bacteria *per se,* as judged by the high degree of coloration due to biliverdin production in *E. coli* cells expressing recombinant bacterial HOs.

SUMMARY

The recent explosion of interest in HO at the physiological level has increased both our awareness of its ever increasing role in biology, as well as the complex nature of the reaction manifold. Although we have made great strides in characterizing HO both structurally and mechanistically, a great number of unanswered questions still remain. In the future, it may be possible to trap crystalline intermediates along the HO pathway that will facilitate and clarify our current understanding of the relationship of structure to function. Advances in understanding regiospecificity, as well as catalysis, will obviously require a greater knowledge of the molecular dynamics and conformational properties of the protein, and hence techniques such as heteronuclear NMR and molecular dynamic calculations should prove to be especially useful in this endeavor.

ACKNOWLEDGMENTS

The author would especially like to thank Paul Ortiz de Montellano for his support and encouragement over the years. It was both a pleasure and privilege to work in the Ortiz de Montellano laboratory alongside Yi Liu and Justin Torpey with whom much of this work is associated. I would also like to thank Tom Poulos, Pierre Moenne-Loccoz, and Tom Loehr for their continued support and collaboration and without whom much of our recent work on the bacterial HOs would not have been possible.

ABBREVIATIONS

BVR, biliverdin reductase; CO, carbon monoxide; 2D, two-dimensional; EPR, electron paramagnetic resonance; heme, iron-protoporphyrin IX irrespective of oxidation or ligation state; HemO, *Neisseriae meningitidis* heme oxygenase; HmuO, *Corynebacterium diphtheriae* heme oxygenase; HO, heme oxygenase; HO-1 and HO-2, heme oxygenase isozymes 1 and 2; H_2O_2, hydrogen peroxide; MCD, magnetic circular dichroism; NMR, nuclear magnetic resonance; PigA, *Pseudomonas aeruginosa* heme oxygenase.

REFERENCES

1. Beale SI. Biosynthesis of open-chain tetrapyrroles in plants, algae, and cyanobacteria. *Ciba Found Symp* 180: 156–168, 1994.
2. Chu GC, Katakura K, Zhang X, Yoshida T, and Ikeda-Saito M. Heme degradation as catalyzed by a recombinant bacterial heme oxygenase (Hmu O) from *Corynebacterium diphtheriae*. *J Biol Chem* 274: 21319–21325, 1999.
3. Cornejo J, Willows RD, and Beale SI. Phytobilin biosynthesis: cloning and expression of a gene encoding soluble ferredoxin-dependent heme oxygenase from *Synechocystis* sp. PCC 6803. *Plant J* 15: 199–107, 1998.
4. Davis SJ, Kurepa J, and Vierstra RD. The *Arabidopsis thaliana* HY1 locus, required for phytochrome-chromophore biosynthesis, encodes a protein related to heme oxygenases. *Proc Natl Acad Sci U S A* 96: 6541–6546, 1999.
5. Davydov RM, Yoshida T, Ikeda-Saito M, and Hoffman BM. Hydroperoxy-heme oxygenase generated by cryoreduction catalyzes the formation of α-mesohydroxyheme as detected by EPR and ENDOR. *J Am Chem Soc* 121: 10656–10657, 1999.
6. Docherty JC, Firneisz GD, and Schacter BA. Methene bridge carbon atom elimination in oxidative heme degradation catalyzed by heme oxygenase and NADPH-cytochrome P-450 reductase. *Arch Biochem Biophys* 235: 657–664, 1984.
7. Docherty JC, Schacter BA, Firneisz GD, and Brown SB. Mechanism of action of heme oxygenase. A study of heme degradation to bile pigment by ^{18}O labeling. *J Biol Chem* 259: 13066–13069, 1984.
8. Frydman RB, Awruch J, Tomaro ML, and Frydman B. Concerning the specificity of heme oxygenase: the enzymatic oxidation of synthetic hemins. *Biochem Biophys Res Commun* 87: 928–935, 1979.
9. Frydman RB, Tomaro ML, Buldain G, Awruch J, Diaz L, and Frydman B. Specificity of heme oxygenase: a study with synthetic hemins. *Biochemistry* 20: 5177–5182, 1981.
10. Fujii H, Dou Y, Zhou H, Yoshida T, and Ikeda-Saito M. Cobalt prophyrin heme oxygenase complex. EPR evidences for the distal heme pocket hydrogen bonding. *J Am Chem Soc* 120: 8251–8252, 1998.
11. Gorst CM, Wilks A, Yeh DC, Ortiz de Montellano PR, and La Mar GN. Solution ^1H NMR investigation of the molecular and electronic structure of the active site of substrate-bound human heme oxygenase: the nature of the distal hydrogen bond donor to bound ligands. *J Am Chem Soc* 120: 8875–8884, 1998.
12. Hernandez G, Wilks A, Paolesse R, Smith KM, Ortiz de Montellano PR, and La Mar GN. Proton NMR investigation of substrate-bound heme oxygenase: evidence for electronic and steric contributions to stereoselective heme cleavage. *Biochemistry* 33: 6631–6641, 1994.
13. Ishikawa K, Takeuchi N, Takahashi S, Matera KM, Sato M, Shibahara S, Rousseau DL, Ikeda-Saito M, and Yoshida T. Heme oxygenase-2. Properties of the heme complex of the purified tryptic fragment of recombinant human heme oxygenase-2. *J Biol Chem* 270: 6345–6350, 1995.
14. Kikuchi A, Park SY, Miyatake H, Sun D, Sato M, Yoshida T, and Shiro Y. Crystal structure of rat biliverdin reductase. *Nat Struct Biol* 8: 221–225, 2001.
15. Kutty RK and Maines MD. Oxidation of heme c derivatives by purified heme oxygenase. Evidence for the presence of one molecular species of heme oxygenase in the rat liver. *J Biol Chem* 257: 9944–9952, 1982.

16. Lagarias JC. The structure of verdohemochrome and its implications for the mechanism of heme catabolism. *Biochim Biophys Acta* 717: 12–19, 1982.
17. Lee-Robichaud P, Wright JN, Akhtar ME, and Akhtar M. Modulation of the activity of human 17 alpha-hydroxylase-17,20-lyase (CYP17) by cytochrome b5: endocrinological and mechanistic implications. *Biochem J* 308: 901–908, 1995.
18. Lightning LK, Huang H, Moenne-Loccoz P, Loehr TM, Schuller DJ, Poulos TL, and Ortiz De Montellano PR. Disruption of an active site hydrogen bond converts human heme oxygenase-1 into a peroxidase. *J Biol Chem* 276: 10612–10619, 2001.
19. Liu Y and Ortiz de Montellano PR. Reaction intermediates and single turnover rate constants for the oxidation of heme by human heme oxygenase-1. *J Biol Chem* 275: 5297–5307, 2000.
20. Liu Y, Moenne-Loccoz P, Loehr TM, and Ortiz de Montellano PR. Heme oxygenase-1, intermediates in verdoheme formation and the requirement for reduction equivalents. *J Biol Chem* 272: 6909–6917, 1997.
21. Liu Y, Koenigs Lightning L, Huang H, Moenne-Loccoz P, Schuller DJ, Poulos TL, Loehr TM, and Ortiz de Montellano PR. Replacement of the distal glycine 139 transforms human heme oxygenase-1 into a peroxidase. *J Biol Chem* 275: 34501–34507, 2000.
22. Maines MD. *Heme Oxygenase: Clinical Applications and Functions*. Boca Raton, FL: CRC Press, 1992.
23. Matera KM, Takahashi S, Fujii H, Zhou H, Ishikawa K, Yoshimura T, Rousseau DL, Yoshida T, and Ikeda-Saito M. Oxygen and one reducing equivalent are both required for the conversion of alpha-hydroxyhemin to verdoheme in heme oxygenase. *J Biol Chem* 271: 6618–6624, 1996.
24. McCoubrey WK Jr, Ewing JF, and Maines MD. Human heme oxygenase-2: characterization and expression of a full-length cDNA and evidence suggesting that the two HO-2 transcripts may differ by choice of polyadenylation signal. *Arch Biochem Biophys* 295: 13–20, 1992.
25. McCoubrey WK, Huang TJ, and Maines MD. Isolation and characterization of a cDNA from the rat brain that encodes hemoprotein heme oxygenase-3. *Eur J Biochem* 247: 725–732, 1997.
26. McDonagh AF. Turning green to gold. *Nat Struct Biol* 8: 198–200, 2001.
27. Migita CT, Matera KM, Ikeda-Saito M, Olson JS, Fujii H, Yoshimura T, Zhou H, and Yoshida T. The oxygen and carbon monoxide reactions of heme oxygenase. *J Biol Chem* 273: 945–949, 1998.
28. Migita CT, Fujii H, Mansfield Matera K, Takahashi S, Zhou H, and Yoshida T. Molecular oxygen oxidizes the porphyrin ring of the ferric alpha-hydroxyheme in heme oxygenase in the absence of reducing equivalent. *Biochim Biophys Acta* 1432: 203–213, 1999.
29. Ortiz de Montellano PR. The mechanism of heme oxygenase. *Curr Opin Chem Biol* 4: 221–227, 2000.
30. Ortiz de Montellano PR and Wilks A. Heme oxygenase structure and mechanism. *Adv Inorg Chem* 51: 359–402, 2000.
31. Pond AE, Roach MP, Sono M, Rux AH, Franzen S, Hu R, Thomas MR, Wilks A, Dou Y, Ikeda-Saito M, Ortiz de Montellano PR, Woodruff WH, Boxer SG, and Dawson JH. Assignment of the heme axial ligand(s) for the ferric myoglobin (H93G) and heme oxygenase (H25A) cavity mutants as oxygen donors using magnetic circular dichroism. *Biochemistry* 38: 7601–7608, 1999.
32. Ratliff M, Zhu W, Stojilijkovic I, and Wilks A. Homologues of neisserial heme oxygenase in gram-negative bacteria: degradation of heme by the product of a pigA gene of *Pseudomonas aeruginosa*. *J Bacteriol* 183: 6394–6403, 2001.
33. Rodriguez JC and Rivera M. Conversion of mitochondrial cytochrome b5 into a species capable of performing the efficient coupled oxidation of heme. *Biochemistry* 37: 13082–13090, 1998.
34. Saito S and Itano HA. Verdohemochrome IX alpha: preparation and oxidoreductive cleavage to biliverdin IX alpha. *Proc Natl Acad Sci U S A* 79: 1393–1397, 1982.
35. Sano S, Sano T, Morishima I, Shiro Y, and Maeda Y. On the mechanism of the chemical and enzymic oxygenations of α-oxyprotohemin IX to Fe. biliverdin IXα. *Proc Natl Acad Sci U S A* 83: 531–535, 1986.
36. Schacter BA, Nelson EB, Marver HS, and Masters BS. Immunochemical evidence for an association of heme oxygenase with the microsomal electron transport system. *J Biol Chem* 247: 3601–3607, 1972.
37. Schmitt MP. Utilization of host iron sources by *Corynebacterium diphtheriae:* identification of a gene whose product is homologous to eukaryotic heme oxygenases and is required for acquisition of iron from heme and hemoglobin. *J Bacteriol* 179: 838–845, 1997.
38. Schuller DJ, Wilks A, Ortiz de Montellano PR, and Poulos TL. Crystal structure of human heme oxygenase-1. *Nat Struct Biol* 6: 860–867, 1999.
39. Schuller DJ, Zhu W, Stojiljkovic I, Wilks A, and Poulos TL. Crystal structure of heme oxygenase from the gram-negative pathogen *Neisseriae meningitidis* and a comparison with mammalian heme oxygenase-1. *Biochemistry* 40: 11552–11558, 2001.
40. Springer BA, Sligar SG, Olson JS, and Phillips GN. Mechanisms of ligand recognition in myoglobin. *Chem Rev* 94: 669–714, 1994.
41. Sugishima M, Omata Y, Kakuta Y, Sakamoto H, Noguchi M, and Fukuyama K. Crystal structure of rat heme oxygenase-1 in complex with heme. *FEBS Lett* 471: 61–66, 2000.
42. Sun J, Wilks A, Ortiz de Montellano PR, and Loehr TM. Resonance Raman and EPR spectroscopic studies on heme–heme oxygenase complexes. *Biochemistry* 32: 14151–14157, 1993.
43. Sun J, Loehr TM, Wilks A, and Ortiz de Montellano PR. Identification of histidine 25 as the heme ligand in human liver heme oxygenase. *Biochemistry* 33: 13734–13740, 1994.
44. Takahashi S, Ishikawa K, Takeuchi E, Ikeda-Saito M, Yoshida T, and Rousseau DL. Oxygen-bound heme–heme oxygenase complex: evidence for a highly bent structure of the coordinated oxygen. *J Am Chem Soc* 117: 6002–6006, 1995.
45. Tenhunen R, Marver HS, and Schmid R. Microsomal heme oxygenase. Characterization of the enzyme. *J Biol Chem* 244: 6388–6394, 1969.

46. Tenhunen R, Marver H, Pimstone NR, Trager WF, Cooper DY, Schmid R. Enzymatic degradation of heme. Oxygenative cleavage requiring cytochrome P450. *Biochemistry* 11: 1716–1720, 1972.
47. Tomaro ML, Frydman RB, Frydman B, Pandey RK, and Smith KM. The oxidation of hemins by microsomal heme oxygenase. Structural requirements for the retention of substrate activity. *Biochim Biophys Acta* 791: 342–349, 1984.
48. Torpey J. Mechanistic studies of heme oxygenase. University of California, San Francisco, Ph.D. Thesis, 1997.
49. Torpey J and Ortiz de Montellano PR. Oxidation of the meso-methylmesoheme regioisomers by heme oxygenase. Electronic control of the reaction regiospecificity. *J Biol Chem* 271: 26067–26073, 1996.
50. Torpey J, Ortiz de Montellano PR. Oxidation of alpha-meso-formylmesoheme by heme oxygenase. Electronic control of the reaction regiospecificity. *J Biol Chem* 272: 22008–22014, 1997.
51. Torpey J, Lee DA, Smith KM, and Ortiz de Montellano PR. Oxidation of an α-meso-methyl-substituted heme to an α-biliverdin by heme oxygenase. A novel heme cleavage reaction. *J Am Chem Soc* 118: 9172–9173, 1996.
52. Wilks A and Moenne-Loccoz P. Identification of the proximal ligand His-20 in heme oxygenase (Hmu O) from *Corynebacterium diphtheriae*. Oxidative cleavage of the heme macrocycle does not require the proximal histidine. *J Biol Chem* 275: 11686–11692, 2000.
53. Wilks A and Ortiz de Montellano PR. Rat liver heme oxygenase. High level expression of a truncated soluble form and nature of the meso-hydroxylating species. *J Biol Chem* 268: 22357–22362, 1993.
54. Wilks A and Schmitt MP. Expression and characterization of a heme oxygenase (Hmu O) from *Corynebacterium diphtheriae*. Iron acquisition requires oxidative cleavage of the heme macrocycle. *J Biol Chem* 273: 837–841, 1998.
55. Wilks A, Torpey J, and Ortiz de Montellano PR. Heme oxygenase (HO-1). Evidence for electrophilic oxygen addition to the porphyrin ring in the formation of alpha-meso-hydroxyheme. *J Biol Chem* 269: 29553–29556, 1994.
56. Wilks A, Black SM, Miller WL, and Ortiz de Montellano PR. Expression and characterization of truncated human heme oxygenase (hHO-1) and a fusion protein of hHO-1 with human cytochrome P450 reductase. *Biochemistry* 34: 4421–4427, 1995.
57. Wilks A, Sun J, Loehr TM, and Ortiz de Montellano PR. Heme oxygenase His25 Ala mutant: replacement of the proximal iron ligand by exogenous bases restores catalytic activity. *J Am Chem Soc* 117: 2925–2926, 1995.
58. Yoshida T and Kikuchi G. Purification and properties of heme oxygenase from pig spleen microsomes. *J Biol Chem* 253: 4224–4229, 1978.
59. Yoshida T and Kikuchi G. Purification and properties of heme oxygenase from rat liver microsomes. *J Biol Chem* 254: 4487–4491, 1979.
60. Yoshida T, Noguchi M, and Kikuchi G. Oxygenated form of heme, heme oxygenase complex and requirement for second electron to initiate heme degradation from the oxygenated complex. *J Biol Chem* 255: 4418–4420, 1980.
61. Zhou H, Migita CT, Sato M, Sun D, Zhang X, Ikeda-Saito M, Fuji H, and Yoshida T. Participation of carboxylate amino acid side chain in regiospecific oxidation of heme by heme oxygenase. *J Am Chem Soc* 122: 8311–8312, 2000.
62. Zhu W, Hunt DJ, Richardson AR, and Stojiljkovic I. Use of heme compounds as iron sources by pathogenic neisseriae requires the product of the hemO gene. *J Bacteriol* 182: 439–447, 2000.
63. Zhu W, Wilks A, and Stojiljkovic I. Degradation of heme in gram-negative bacteria: the product of the hemO gene of Neisseriae is a heme oxygenase. *J Bacteriol* 182: 6783–6790, 2000.

Address reprint requests to:
Angela Wilks
Department of Pharmaceutical Sciences
School of Pharmacy
University of Maryland
20 North Pine Street
Baltimore, MD 21201–1180

E-mail: awilks@rx.umaryland.edu

Received for publication May 11, 2001; accepted January 4, 2002.

This article has been cited by:

1. Dungeng Peng, Li-Hua Ma, Kevin M. Smith, Xuhong Zhang, Michihiko Sato, Gerd N. La Mar. 2012. Role of Propionates in Substrate Binding to Heme Oxygenase from Neisseria meningitidis : A Nuclear Magnetic Resonance Study. *Biochemistry* **51**:36, 7054-7063. [CrossRef]
2. Magnus G. Olsson , Maria Allhorn , Leif Bülow , Stefan R. Hansson , David Ley , Martin L. Olsson , Artur Schmidtchen , Bo Åkerström . 2012. Pathological Conditions Involving Extracellular Hemoglobin: Molecular Mechanisms, Clinical Significance, and Novel Therapeutic Opportunities for #1-Microglobulin. *Antioxidants & Redox Signaling* **17**:5, 813-846. [Abstract] [Full Text HTML] [Full Text PDF] [Full Text PDF with Links]
3. Sheng Xu, Lijuan Wang, Bo Zhang, Bin Han, Yanjie Xie, Jie Yang, Weigong Zhong, Huiping Chen, Ren Wang, Ning Wang, Weiti Cui, Wenbiao Shen. 2012. RNAi knockdown of rice SE5 gene is sensitive to the herbicide methyl viologen by the down-regulation of antioxidant defense. *Plant Molecular Biology* . [CrossRef]
4. M. Indriati Hood, Eric P. Skaar. 2012. Nutritional immunity: transition metals at the pathogen–host interface. *Nature Reviews Microbiology* **10**:8, 525-537. [CrossRef]
5. Anna Grochot#Przeczek, Jozef Dulak, Alicja Jozkowicz. 2012. Haem oxygenase-1: non-canonical roles in physiology and pathology. *Clinical Science* **122**:3, 93-103. [CrossRef]
6. Bin Han, Sheng Xu, Yan-Jie Xie, Jing-Jing Huang, Li-Juan Wang, Zheng Yang, Chang-He Zhang, Ya Sun, Wen-Biao Shen, Gui-Shui Xie. 2011. ZmHO-1, a maize haem oxygenase-1 gene, plays a role in determining lateral root development. *Plant Science* . [CrossRef]
7. Dungeng Peng, James D Satterlee, Li-Hua Ma, Jerry L Dallas, Kevin Malcolm Smith, Xuhong Zhang, Michihiko Sato, Gerd Neustadter La Mar. 2011. Influence of substrate modification and C-terminal truncation on the active site structure of substrate-bound heme oxygenase from Neisseriae meningitidis; A ¹H NMR study. *Biochemistry* 110827140832039. [CrossRef]
8. A. Gaballa, J. D. Helmann. 2011. Bacillus subtilis Fur represses one of two paralogous heme-degrading monooxygenases. *Microbiology* . [CrossRef]
9. Yanjie Xie, Weiti Cui, Xingxing Yuan, Wenbiao Shen, Qing Yang. 2011. Haem Oxygenase-1 is Associated with Wheat Salinity Acclimation by Modulating Reactive Oxygen Species Homeostasis. *Journal of Integrative Plant Biology* no-no. [CrossRef]
10. M. Wu, J. Huang, S. Xu, T. Ling, Y. Xie, W. Shen. 2011. Haem oxygenase delays programmed cell death in wheat aleurone layers by modulation of hydrogen peroxide metabolism. *Journal of Experimental Botany* **62**:1, 235-248. [CrossRef]
11. Christopher L. Nobles, Anthony W. Maresso. 2011. The theft of host heme by Gram-positive pathogenic bacteria. *Metallomics* . [CrossRef]
12. C.D. Caiaffa, R. Stiebler, M.F. Oliveira, F.A. Lara, G.O. Paiva-Silva, P.L. Oliveira. 2010. Sn-protoporphyrin inhibits both heme degradation and hemozoin formation in Rhodnius prolixus midgut. *Insect Biochemistry and Molecular Biology* **40**:12, 855-860. [CrossRef]
13. Wenzhen Lai, Hui Chen, Toshitaka Matsui, Kohei Omori, Masaki Unno, Masao Ikeda-Saito, Sason Shaik. 2010. Enzymatic Ring-Opening Mechanism of Verdoheme by the Heme Oxygenase: A Combined X-ray Crystallography and QM/MM Study. *Journal of the American Chemical Society* **132**:37, 12960-12970. [CrossRef]
14. G. S. Shekhawat, K. Verma. 2010. Haem oxygenase (HO): an overlooked enzyme of plant metabolism and defence. *Journal of Experimental Botany* **61**:9, 2255-2270. [CrossRef]
15. Michelle L. Reniere, Georgia N. Ukpabi, S. Reese Harry, Donald F. Stec, Robert Krull, David W. Wright, Brian O. Bachmann, Michael E. Murphy, Eric P. Skaar. 2010. The IsdG-family of haem oxygenases degrades haem to a novel chromophore. *Molecular Microbiology* **75**:6, 1529-1538. [CrossRef]

16. Raffaella Gozzelino, Viktoria Jeney, Miguel P. Soares. 2010. Mechanisms of Cell Protection by Heme Oxygenase-1. *Annual Review of Pharmacology and Toxicology* **50**:1, 323-354. [CrossRef]
17. Bjoern Gisk, Yukiko Yasui, Takayuki Kohchi, Nicole Frankenberg#Dinkel. 2010. Characterization of the haem oxygenase protein family in Arabidopsis thaliana reveals a diversity of functions. *Biochemical Journal* **425**:2, 425-434. [CrossRef]
18. Cheng Li, Roland Stocker. 2009. Heme oxygenase and iron: from bacteria to humans. *Redox Report* **14**:3, 95-101. [CrossRef]
19. Miguel P. Soares, Fritz H. Bach. 2009. Heme oxygenase-1: from biology to therapeutic potential. *Trends in Molecular Medicine* **15**:2, 50-58. [CrossRef]
20. Yong Tong, Maolin Guo. 2009. Bacterial heme-transport proteins and their heme-coordination modes. *Archives of Biochemistry and Biophysics* **481**:1, 1-15. [CrossRef]
21. Agnieszka Loboda , Agnieszka Jazwa , Anna Grochot-Przeczek , Andrzej J. Rutkowski , Jaroslaw Cisowski , Anupam Agarwal , Alicja Jozkowicz , Jozef Dulak . 2008. Heme Oxygenase-1 and the Vascular Bed: From Molecular Mechanisms to Therapeutic Opportunities. *Antioxidants & Redox Signaling* **10**:10, 1767-1812. [Abstract] [Full Text PDF] [Full Text PDF with Links]
22. Shih-Long Tu, Clark LagariasThe Phytochromes . [CrossRef]
23. Mehul N. Bhakta, Ayodele Olabisi, Kandategе Wimalasena, Angela Wilks. 2008. Catalytic turnover dependent modification of the Pseudomonas aeruginosa heme oxygenase (pa-HO) by 5,6-O-isopropyledine-2-O-allyl-ascorbic acid. *Journal of Inorganic Biochemistry* **102**:2, 251-259. [CrossRef]
24. Thorben Dammeyer, Nicole Frankenberg-Dinkel. 2008. Function and distribution of bilin biosynthesis enzymes in photosynthetic organisms. *Photochemical & Photobiological Sciences* **7**:10, 1121. [CrossRef]
25. Daniel A. Landfried, David A. Vuletich, Matthew P. Pond, Juliette T.J. Lecomte. 2007. Structural and thermodynamic consequences of b heme binding for monomeric apoglobins and other apoproteins. *Gene* **398**:1-2, 12-28. [CrossRef]
26. Martin Bröring, Stephan Link, Carsten D. Brandt, Esther Cónsul Tejero. 2007. Helical Transition-Metal Complexes of Constrained 2,2#-Bidipyrrins. *European Journal of Inorganic Chemistry* **2007**:12, 1661-1670. [CrossRef]
27. Ulf Lindh. 2007. Metal Biology: Aspects of Beneficial Effects. *AMBIO: A Journal of the Human Environment* **36**:1, 107-110. [CrossRef]
28. Masaki Unno, Toshitaka Matsui, Masao Ikeda-Saito. 2007. Structure and catalytic mechanism of heme oxygenase. *Natural Product Reports* **24**:3, 553. [CrossRef]
29. Angela Wilks, Kimberly A. Burkhard. 2007. Heme and virulence: how bacterial pathogens regulate, transport and utilize heme. *Natural Product Reports* **24**:3, 511. [CrossRef]
30. Philip J. Linley, Martin Landsberger, Takayuki Kohchi, Jon B. Cooper, Matthew J. Terry. 2006. The molecular basis of heme oxygenase deficiency in the pcd1 mutant of pea. *FEBS Journal* **273**:12, 2594-2606. [CrossRef]
31. B SEHRINGER, H KAYSER. 2006. Butterfly wings, a new site of porphyrin synthesis and cleavage: Studies on the expression of the lipocalin bilin-binding protein in Pieris brassicae. *Insect Biochemistry and Molecular Biology* **36**:6, 482-491. [CrossRef]
32. A. W. Maresso, Olaf Schneewind. 2006. Iron Acquisition and Transport in Staphylococcus aureus. *BioMetals* **19**:2, 193-203. [CrossRef]
33. Anne Blumenstein, Kay Vienken, Ronja Tasler, Janina Purschwitz, Daniel Veith, Nicole Frankenberg-Dinkel, Reinhard Fischer. 2005. The Aspergillus nidulans Phytochrome FphA Represses Sexual Development in Red Light. *Current Biology* **15**:20, 1833-1838. [CrossRef]
34. Latesh Lad, Paul R. Ortiz de Montellano, Thomas L. Poulos. 2004. Crystal structures of ferrous and ferrous–NO forms of verdoheme in a complex with human heme oxygenase-1: catalytic implications for heme cleavage. *Journal of Inorganic Biochemistry* **98**:11, 1686-1695. [CrossRef]

35. Michael L Pendrak, S.Steve Yan, David D Roberts. 2004. Sensing the host environment: recognition of hemoglobin by the pathogenic yeast Candida albicans. *Archives of Biochemistry and Biophysics* **426**:2, 148-156. [CrossRef]

36. Stefan W. Ryter, Leo E. Otterbein. 2004. Carbon monoxide in biology and medicine. *BioEssays* **26**:3, 270-280. [CrossRef]

37. Eric P. Skaar, Olaf Schneewind. 2004. Iron-regulated surface determinants (Isd) of Staphylococcus aureus: stealing iron from heme. *Microbes and Infection* **6**:4, 390. [CrossRef]

38. H Pae. 2003. Differential expressions of heme oxygenase-1 gene in CD25- and CD25+ subsets of human CD4+ T cells. *Biochemical and Biophysical Research Communications* **306**:3, 701-705. [CrossRef]

39. Jawed Alam . 2002. Heme Oxygenase-1: Past, Present, and Future. *Antioxidants & Redox Signaling* **4**:4, 559-562. [Citation] [Full Text PDF] [Full Text PDF with Links]